



# Study on the composition, microstructure and mechanical properties of PCBN composites synthesized by TiN–AlN–Ti combined with cBN

Peicheng Mo<sup>1,2,\*</sup> , Jiarong Chen<sup>1,2</sup>, Chao Chen<sup>1,2</sup>, Qiaofan Hu<sup>1,2</sup>, Xiaoyi Pan<sup>1,2</sup>, Leyin Xiao<sup>1,2</sup>, and Feng Lin<sup>1,2</sup>

<sup>1</sup>Guangxi Key Laboratory of Superhard Material, China Nonferrous Metal (Guilin) Geology and Mining Co., Ltd., Guilin 541004, Guangxi, China

<sup>2</sup>National Engineering Research Center for Special Mineral Material, China Nonferrous Metal (Guilin) Geology and Mining Co., Ltd., Guilin 541004, Guangxi, China

Received: 16 June 2022

Accepted: 7 September 2022

Published online:

19 September 2022

© The Author(s), under exclusive licence to Springer Science+Business Media, LLC, part of Springer Nature 2022

## ABSTRACT

Polycrystalline cubic boron nitride (PCBN) was synthesized at high temperature and ultra-high pressure, using cBN, TiN, AlN and Ti as starting materials. The effects of CBN content (48–63 wt%) and sintering temperature (1300–1600 °C) on the composition, microstructure and mechanical properties of PCBN materials were studied. X-ray diffraction and scanning electron microscope were used to analyze the phase composition, microstructure and surface crack morphology of PCBN. At the same time, the compactness, microhardness, fracture toughness and flexural strength of PCBN were tested. Research shows that the phase components of PCBN samples are mainly composed of BN, TiB<sub>2</sub>, TiN and AlN. Almost all Ti reacts with cBN during the sintering process to form TiN and TiB<sub>2</sub> phases. When the sintering temperature is 1500 °C, the reaction has been fully completed. When the cBN content increases from 48 to 63 wt%, the relative density, flexural strength and hardness of PCBN increase with the increase in cBN content. When sintered at 1500 °C and the cBN content is 63 wt%, the relative density, flexural strength, fracture toughness and microhardness of the composite are 99%, 820.8 MPa, 6.6 MPa·m<sup>1/2</sup> and 3362 Hv, respectively.

Handling Editor: Catalin Croitoru.

Address correspondence to E-mail: 2393707540@qq.com

<https://doi.org/10.1007/s10853-022-07726-3>

## Introduction

With the rapid development of modern technology, a large number of difficult-to-process materials have appeared while the performance of workpiece materials has been improved and improved. These materials have high requirements for machining accuracy and technical conditions. Traditional tools (such as high-speed steel, cemented carbide and ceramic tools) cannot meet the needs of parts processing, but the emergence of superhard materials has solved this problem. Utilizing the characteristics of high hardness, high wear resistance, high thermal conductivity, low friction and low thermal expansion of superhard tools, it can cut various chilled and hard-to-machine materials [1–3]. For example, Fiorini et al. [4] studied the processing of GG25 gray cast iron by PCBN tool at high cutting speed ( $v_c = 750$  m/min); Gutnichenko et al. [5] used PCBN tools to turn high-chromium white cast iron and carried out related research on tool wear and machining dynamics; Ren et al. [6] studied the machining performance of PCBN tool dry-turned titanium alloys and characterized tool life and surface integrity; Diaz-avarez [7] and Chen et al. [8] performed high-speed turning of Inconel 718 steel and AD 730<sup>TM</sup> steel with PCBN tools, respectively. All the above results show that the PCBN tool has excellent cutting performance. Among them, polycrystalline cubic boron nitride (PCBN) tools are the most typical, and PCBN tools have higher hardness and wear resistance than ceramic and carbide tools. In addition, it has excellent thermal stability, thermal conductivity and chemical stability. It plays a key role in modern machining and becomes an indispensable tool [9–11].

PCBN is synthesized from cubic boron nitride and binder under high temperature and high pressure. The binder plays an important role in the synthesis process. Adding an appropriate amount of the binder can reduce the sintering temperature and pressure, while improving the properties of the sintered body. Binders are divided into metal binders and ceramic binders. Metal binders mainly include Co, Al, Ti and Ni, etc. [12–17]. They chemically bond with cBN under high temperature and high pressure to sinter into PCBN. Ceramic binders are mainly nitrides, borides and carbides of aluminum and titanium. Although they are not as violent as metals when they chemically react with cBN, they can be sintered into

PCBN by mutual infiltration under ultra-high pressure and high temperature [18, 19]. Among various metal and ceramic bonding agents, metal Ti and high melting point compound TiN are often used as the main bonding agent to combine with cBN to obtain PCBN tool materials with excellent comprehensive properties. Ti has very active chemical properties and can react with cBN to form TiN and TiB<sub>2</sub>, which can enhance the thermal stability, red hardness and fracture toughness of PCBN [14, 19]. The addition of TiN can effectively improve the thermal stability of PCBN composites, and at the same time, it can participate in high-speed cutting as a hard phase. The high thermal conductivity of AlN is conducive to the heat dissipation of the composite material and reduces the interface thermal stress [2]. At the same time, AlN is also a catalyst for the conversion of hBN to cBN, which can effectively inhibit the phase change of cBN.

In recent years, the research on PCBN materials has made great progress. Lili et al. [20] used Hf-Al as binder to prepare PCBN material with uniform structure and good wear resistance under HPHT. Mingliang et al. [21] used PSN and Al as sintering additives to prepare PCBN materials with a relative density of 99.7%, a Vickers hardness of 25.2 GPa and a bending strength of 602 MPa. Peicheng et al. [22] used Ti/Al/Si as a binder to synthesize a PCBN material with a microhardness of 34.58 GPa, a flexural strength of 799 MPa, a porosity of 0.21% and a relative density of 98.5%. Yuan et al. [23] used the cBN-Ti-Al composite was prepared by spark plasma sintering. The composite with optimal mechanical properties was prepared for 1400 °C, and the relative density, the bending strength and hardness were  $98.9 \pm 0.1\%$ ,  $390.7 \pm 4.4$  MPa and  $14.1 \pm 0.5$  GPa, respectively. Different binders affect different properties of PCBN materials. In order to obtain high-strength, high-toughness PCBN, this paper chooses TiN as the main binder, adding certain amount of AlN and Ti. Optimize the assembly structure and the corresponding sintering process under high-temperature and high-pressure (HPHT) conditions. The effects of CBN content (48–63 wt%) and sintering temperature (1300–1600 °C) on the composition, microstructure and mechanical properties of PCBN composites synthesized by TiN–AlN–Ti combined with cBN sintering were studied, in order to obtain PCBN composite tool materials containing ceramic

phase, high performance and high stability by sintering.

## Experiment

### Sample preparation

cBN (particle size 1–3  $\mu\text{m}$ , purity 99.9%, Funike Superhard Materials Co., Ltd. China), TiN (particle size 1–2  $\mu\text{m}$ , purity 99.9%, Wuxi Edma Technology Co., Ltd. China) AlN (particle size 1–2  $\mu\text{m}$ , purity 99.9%, Shanghai Aladdin Biochemical Technology Co., Ltd. China), Ti (particle size 1–2  $\mu\text{m}$ , purity 99.9%, Shanghai Aladdin Biochemical Technology Co., Ltd. China), as experimental raw materials. Make ingredients according to Table 1, among them, TiN:Ti:AlN = 15:8:2 (wt%) in the binder. Use n-heptane (purity 99.5%, Shanghai Aladdin Biochemical Technology Co., Ltd. China) and alcohol (purity 99.5%, Shanghai Aladdin Biochemical Technology Co., Ltd. China) as the medium in a stainless steel ball milling; the volume ratio is 1:1. Carbide balls with a diameter of 5  $\mu\text{m}$  were added, the ball-to-material ratio was 4:1, and the ball milling speed was 300  $\text{r}\cdot\text{min}^{-1}$ ; grind the mixture for 2 h, and then dry it in a drying oven at 100  $^{\circ}\text{C}$  for 6 h. Put the mixed powder into a cylindrical molybdenum cup with a diameter of 35 mm, and then pre-compress it into a block on a cold press forming machine. After being treated by a high-temperature vacuum at 800  $^{\circ}\text{C}$ , it is put into a pyrophyllite mold. Then it is sintered at high temperature and ultra-high pressure in a hinged six-sided top press. The sintering temperature is 1300–1600  $^{\circ}\text{C}$  ( $\pm 10$   $^{\circ}\text{C}$ ), the pressure during sintering is 5.5 GPa, and the holding time is 700 s.

### Performance characterization

Grind and polish the PCBN sample on a diamond automatic polishing machine to a matte surface; use

**Table 1** Composition details of the experiment

No	cBN (wt%)	Binder (wt%)
TA1	48	52
TA2	53	47
TA3	58	42
TA4	63	37

X-ray diffraction (model: X'pert PRO) to analyze the phase composition of PCBN samples; use Archimedes drainage method to determine the relative density and porosity of PCBN samples; use S-4800 field emission scanning electron microscope (SEM) to characterize the microstructure, crystal grain morphology and cross-sectional morphology of PCBN; a microcomputer-controlled electronic universal material testing machine (model CMT-4304) was used to test the flexural strength of the sample, with a span of 10 mm and a loading speed of 0.5 mm/min. The microhardness and fracture toughness were measured by a Vickers microhardness tester (model MH-6) with a loading load of 198 N (20 kg) and a pressure holding time of 15 s. Measure the length of the indentation diagonal and the length of the indentation crack in the Vickers hardness test; Figure 1 shows the indentation crack diagram.

Then calculate the microhardness and fracture toughness of the sample by formula (1) and formula (2), respectively [2, 24].

$$Hv = \frac{1.854P}{d^2} \quad (1)$$

$$KIC = 0.035 \left( \frac{Hv}{E} \right)^{-2/5} \left( \frac{c}{a} - 1 \right)^{-1/2} Hv \sqrt{af^{-3/5}} \quad (2)$$

where  $P$  is the applied load (kgf),  $d$  is the average value of two diagonal lengths from Vickers indentations (mm) and  $E$  is the Young's modulus of the cBN-based composites. Calculate according to the mixture rule (GPa);  $Hv$  is the hardness (GPa);  $a$  is the half length of the indent diagonal (mm);  $c$  is the half-crack

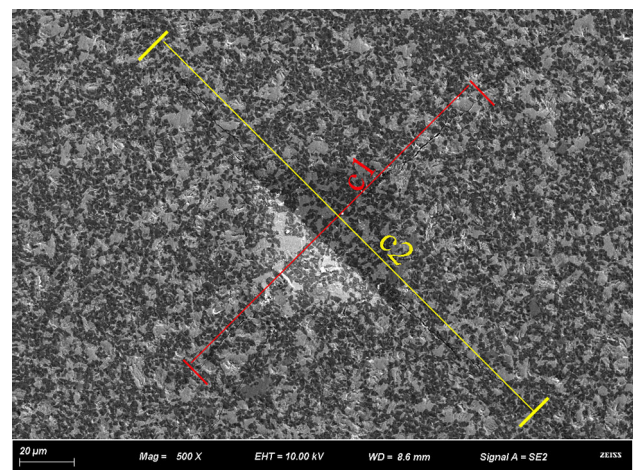


**Figure 1** The indentation crack diagram.

length from the center of the indent to tip of the crack (mm); and  $f$  is a constraint factor (equal to 3) [2].

$E$  is calculated according to formula (3) in PCBN sintered body:

$$E = \sum E_i f_i \quad (3)$$

In the formula,  $E_i$  represents the Young's modulus of each component of PCBN, and  $f_i$  represents the volume fraction of each component of PCBN.

## Result analysis

### Physical analysis

Figure 2 XRD patterns of PCBN samples with different percentages of cBN added at 1500 °C. It can be seen from the figure that in the PCBN sintered body obtained after high-temperature and ultra-high pressure sintering, there is no obvious difference in product types, and they are all composed of BN, TiB<sub>2</sub>, TiN and AlN. The presence of metallic titanium was not detected in the XRD pattern, indicating that a chemical reaction occurred between elemental titanium and cBN, resulting in the formation of new phases TiB<sub>2</sub> and TiN. TiB<sub>2</sub> has high hardness, excellent thermal stability and excellent wear resistance, so it can improve the toughness and strength of PCBN composites. Because the added AlN can inhibit the phase transition from cBN to hBN, the presence of hBN is not detected in the XRD pattern. At the same time, no other impurity phases were detected in the

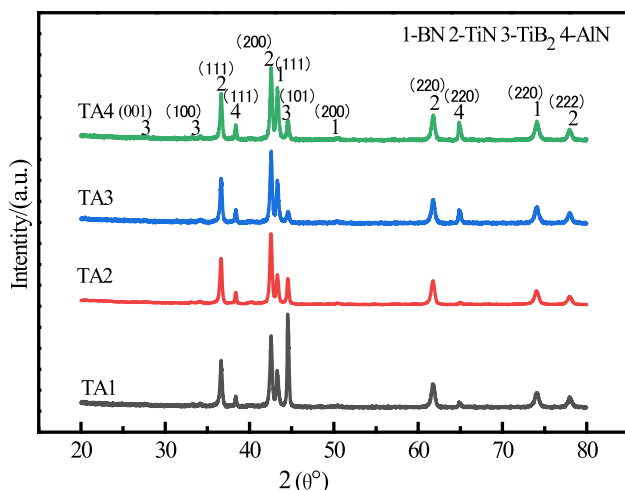


**Figure 2** XRD of PCBN samples with different CBN percentage content added at 1500 °C.

XRD spectrum. On the one hand, it shows that the purity of the powder is good. On the other hand, it also shows that the mixing process is reasonable, and the cemented carbide balls and the cemented carbide tank base material are rarely dropped off. The impurity contained in PCBN will reduce the strength and heat resistance of the sintered body, which is the main cause of chipping and wear. The PCBN synthesized in this experiment reduces the impurity to a minimum, improves the heat resistance, and obtains obdurability

### Microstructure analysis

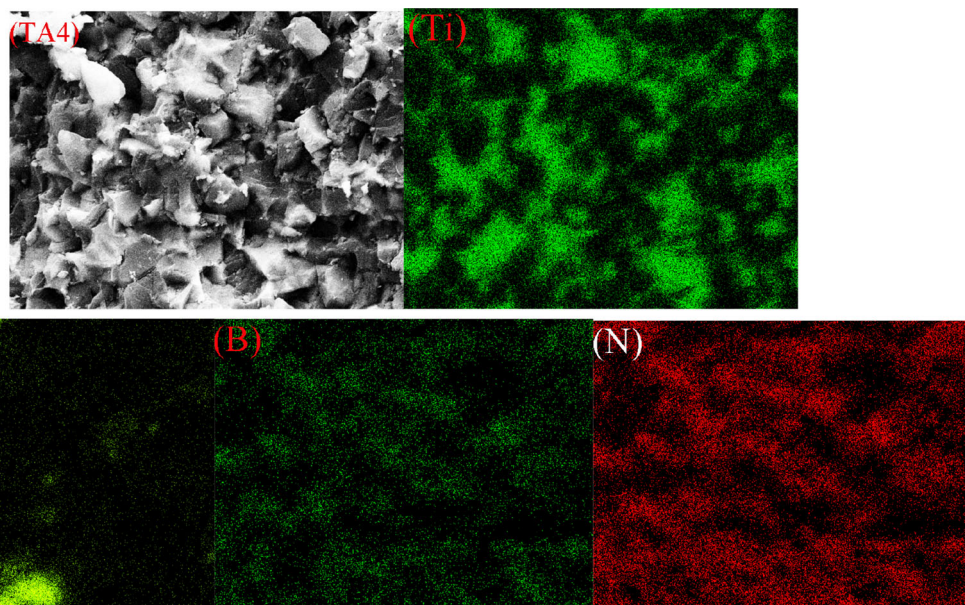
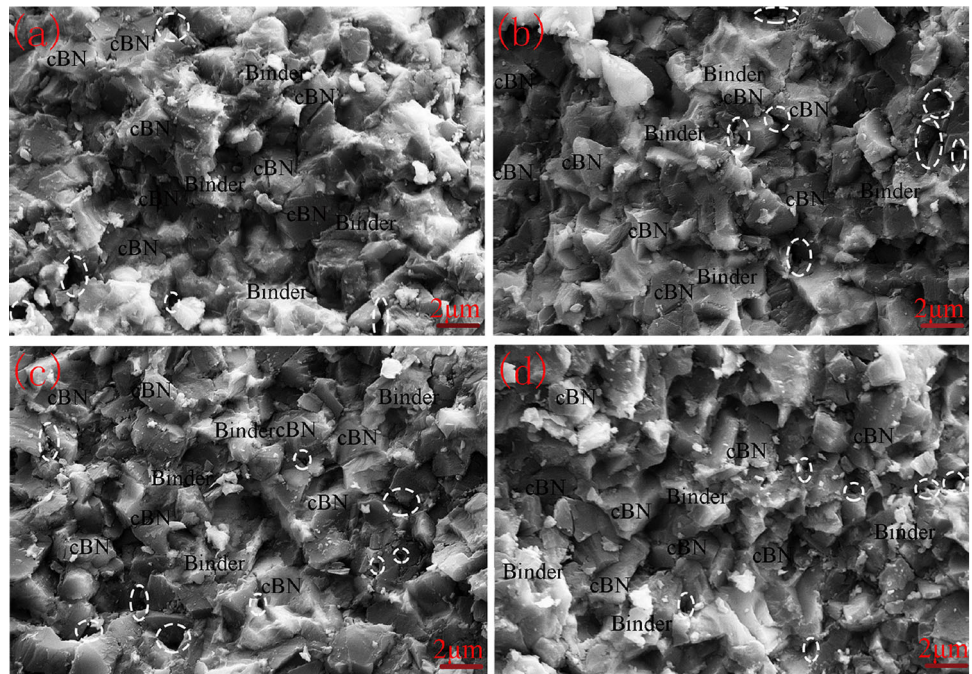
Figure 3 shows the micromorphology of PCBN composites with different cBN content at 1500 °C. The distribution of binding agent and cBN particles can be clearly seen from the figure. In the low-content cBN samples, the binding agent can be observed to aggregate together, and some pores can be observed (shown in the ellipse). As the content of cBN increases, the aggregation state of the binder gradually weakens, the internal pores are also reduced, and the sample becomes denser. The cBN particles are wrapped by a binder, which affects the connection between the cBN particles and plays a key role in strengthening the cBN-based composites. At the same time, some cBN particles are directly combined with each other, indicating that cBN-cBN bonds are formed between different particles during the sintering process, and the pores are more likely to disappear. It can be seen from the observation that obvious grain boundaries and smooth crystal planes can be observed in the figure, and the interfacial bonding force between cBN and the binder is strong.

Figure 4 EDS analysis results of T4 sample at 1500 °C. It can be seen from the figure that the cBN particles are distributed around the binder and are bound together by the binder. BN and TiN/TiB<sub>2</sub> can be uniformly distributed inside the sample, while AlN has partial agglomeration, which may be caused by uneven mixing

Figure 5 shows the microscopic morphology of samples at different sintering temperatures. When the TA4 sample was sintering at low temperature, a large gap was observed between the bonding agent and cBN, the bonding agent was looser, the melting property was poor, the bonding property was poor at low temperatures, and the strength and hardness of the sample will be low. At low temperatures, the



**Figure 3** SEM of PCBN composites with different cBN content at 1500 °C: **a** 52 wt% binder, **b** 47 wt% binder, **c** 42 wt% binder and **d** 37 wt% binder.



**Figure 4** EDS analysis results of T4 sample at 1500 °C.

binder cannot completely sinter and retain the particles. When the temperature rises, the binding force between the binder and cBN increases, and the sample density increases. This compactness contributes to the improvement of the mechanical strength of the PCBN. Under HPHT conditions, some edges and corners of cBN particles become rounded due to the chemical dissolution and reaction between cBN and Ti.

### Analysis of compactness and flexural strength

It can be seen from Fig. 6 that when the content of cBN increases from 48 wt% to 63 wt%, the relative density increases with the increase in the content of cBN. When the content of cBN is lower and the content of binder is higher, the binder will aggregate together in the molten state. Produce more pores,

**Figure 5** SEM of TA4 samples at different sintering temperatures: **a** 1300 °C, **b** 1400 °C, **c** 1500 °C, **d** 1600 °C.

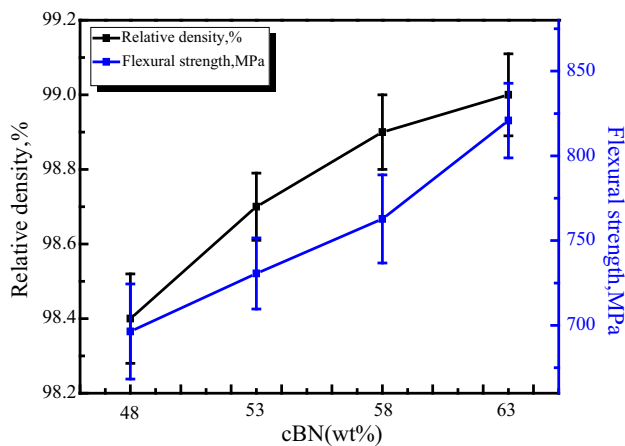
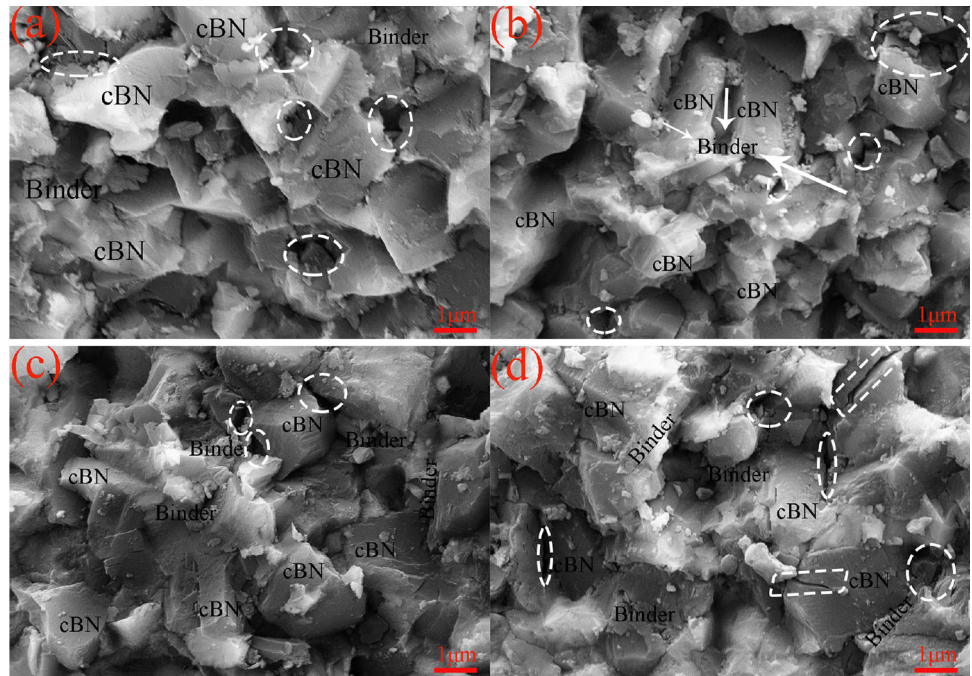


**Figure 6** Relationship between relative density and bending strength of PCBN samples at 1500 °C.

thereby reducing its compactness. With the increase in cBN, this phenomenon will be improved, and the relative density of PCBN samples will gradually increase. The flexural strength increases with the increase in cBN content. When the content of the binder is too much, a molten glass phase is formed during the sintering process, and the low strength of the glass phase will reduce the overall bending strength of the PCBN composite. The bending fracture of the material is the result of crack propagation and the result of the combined action of normal stress and shear stress. When the cBN content increases

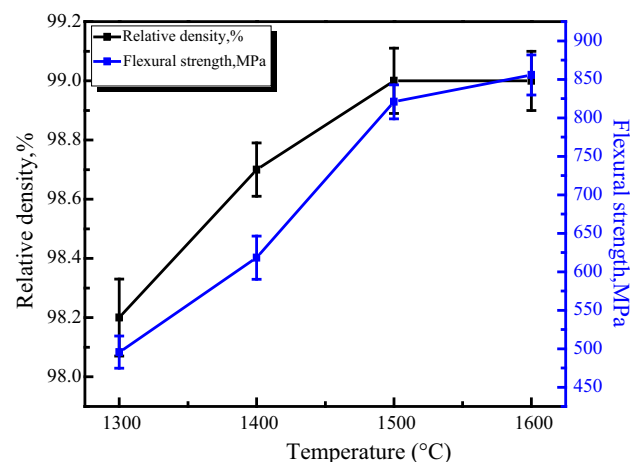


**Figure 7** Relative density and bending strength of TA4 samples at different temperatures.

from 48 to 63 wt%, the number of cBN particles inside the PCBN sintered body is continuously increasing. The increase in cBN particles is beneficial to resist the expansion of internal cracks during the fracture process, so that the cracks will branch during the expansion process and deflection phenomenon, so as to play the role of grain strengthening and obtain higher bending strength.

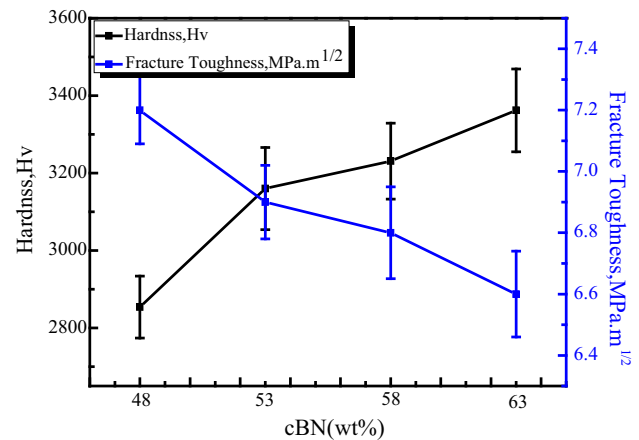
Figure 7 shows the relationship between the relative density and bending strength of the TA4 sample and the sintering temperature. As the sintering temperature increases, the relative density of the sample



increases rapidly and gradually stabilizes at 1500 °C. When the sintering temperature is low, the energy obtained inside the sintered body is less, and the bonding agent may not penetrate into the cBN particles, or it may become molten and flow in the system, which is not conducive to the uniform distribution of the bonding agent and cBN grains. As a result, cBN is in contact with each other during the sintering process, and it is easy to form a bridging phenomenon, produce gaps, and reduce the degree of densification of the PCBN composite material. From the results of the compactness test, it can be seen that when the sintering temperature is 1300 °C, there are many pores inside the PCBN. The existence of pores hinders the connection between the reinforcement phase and the matrix, decreased the effective cross-sectional area of the applied load, and reduces the stress that the sample can withstand. This causes the sample to fracture at lower stress, resulting in lower strength [25, 26]. As the temperature increases, the diffusion rate of the liquid phase inside the material increases, and the higher the energy provided, accelerates the reaction rate of titanium and cBN, and can quickly fill the internal pores, and the structure tends to be dense, which increases the compactness of the sample. The bending strength and relative density curves show a similar trend. As the temperature increases, the increase in relative density increases the bending strength.

### Analysis of microhardness and fracture toughness

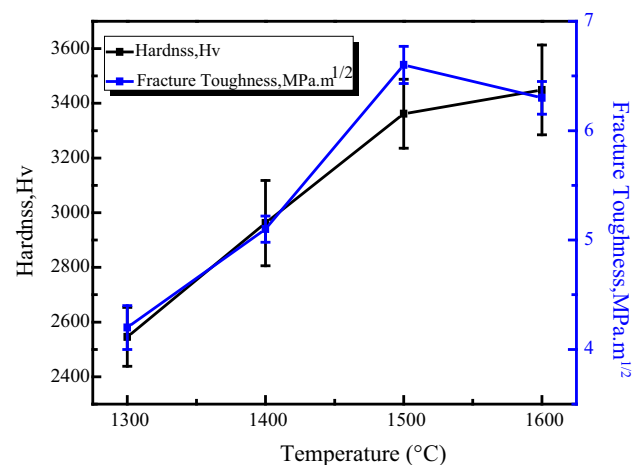
Figure 8 shows the hardness and fracture toughness diagrams of samples with different cBN content. The hardness and fracture toughness were measured by the Vickers indentation method with a load of 198 N (20 kg). For each sample, perform 5 indentation tests. It can be seen from the figure that the hardness of PCBN composite material increases significantly with the increase in cBN content. The type and content of phases in this experiment are the main factors affecting hardness. Among them, the hardness of cBN reaches 80 GPa and the hardness of TiN reaches 30 GPa. There is a big difference in hardness between the two, and the content of cBN in all samples is the largest, and the hardness is also the largest in the phase. Therefore, cBN is the main factor affecting the hardness of PCBN samples. The higher the cBN content, the higher the overall hardness of the



**Figure 8** Relationship between microhardness and cBN content of PCBN sample at 1500 °C.

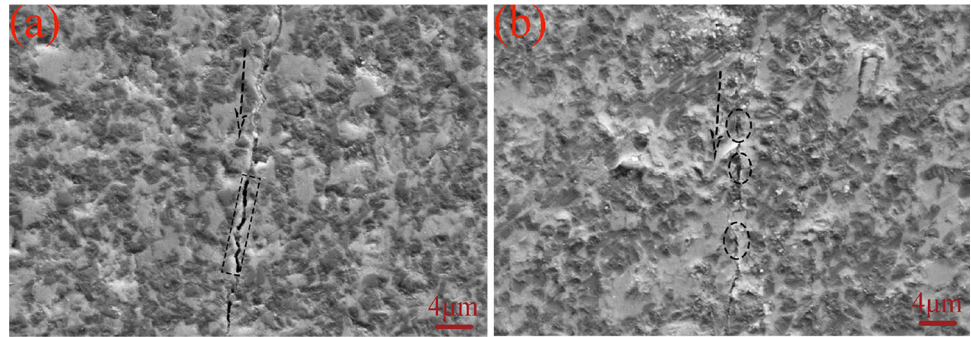
composite material. The toughness value of cBN-based composites with 52 wt% binder is the largest, which is 7.2 MPa.m<sup>1/2</sup>. At a relatively high binder content, it fully reacts with cBN to provide the best toughness of the composite.

Figure 9 shows the hardness and fracture toughness curves of TA4 samples at different temperatures. The fracture toughness of the samples first increases and then decreases as the temperature rises. When the temperature is 1500 °C, the fracture toughness of the TA4 sample is the largest, reaching 6.6 MPa.m<sup>1/2</sup>. The fracture toughness of the sample is related to the relative density, hardness and internal enhancement. TiB<sub>2</sub> generated by the in situ reaction is beneficial to the improvement of fracture toughness. The interface between TiB<sub>2</sub> and cBN is clean and well bonded. When the sample is subjected to an external load,



**Figure 9** Hardness and fracture toughness of TA4 sample at different temperature.

**Figure 10** Crack morphology of TA4 samples at different temperatures.



good interface bonding can carry greater load. At the same time, the thermal expansion coefficients of cBN and  $\text{TiB}_2$ ,  $\text{TiN}$  and  $\text{AlN}$  phases are inconsistent. The sintering and cooling process will cause thermal mismatch, generate residual stress, and form micro-cracks, which play a role in toughening [27]. At the same time, it can be seen from the figure that the microhardness of the sample is also closely related to the sintering temperature. The sample is not completely sintered at low temperatures, contains more intermediate phases, is loose inside and has more pores. The indenter of the Vickers hardness tester is on the pores. The large area occupied makes the sintered body produce larger plastic deformation, resulting in lower hardness. As the temperature rises to 1500 °C, the sample is sintered completely, the phase is stable, and the hardness is higher. From our experimental results, the sintering temperature also has an important influence on the hardness of HPHT-sintered samples.

Figure 10 shows the fracture crack morphology of TA4 samples at different temperatures. It can be seen from the figure that when the sintering temperature is 1400 °C (Fig. 10a), the fracture cracks of the sample mainly split along the gray phase, the cracks are relatively wide and the crack path is relatively straight, and the crack propagation process is not hindered, so the fracture toughness is relatively low. When the sintering temperature is increased to 1500 °C (Fig. 10b), the fracture toughness of the material reaches a maximum of  $6.6 \text{ MPa}\cdot\text{m}^{1/2}$ . The fracture cracks split along the gray phase, passing through part of the black hard phase, and the black phase hinders the further expansion of the crack. The slight deflection of the crack is beneficial to the improvement of the fracture toughness of the material, and the crack is much smaller than the sample

sintered at 1400 °C. As the sintering temperature increases, the density of the material increases, and the size of the hard phase particles increases within a certain range, which is beneficial to deflect the cracks and improve the fracture toughness. However, the increase in the pore size is not conducive to the improvement of the fracture toughness of the material, so as the sintering temperature further increases, the fracture toughness of the material decreases.

## Conclusion

- (1) The phase components of PCBN samples are mainly composed of BN,  $\text{TiB}_2$ ,  $\text{TiN}$  and  $\text{AlN}$ , under different conditions.
- (2) When the cBN content increases from 48 to 63 wt%, the relative density, bending strength and microhardness increase with the increase in cBN content and tend to be stable.
- (3) As the sintering temperature increases, the relative density, flexural strength and microhardness of the sample increase and gradually become stable. At 1500 °C, the relative density did not increase any more, indicating that the inside of the system had fully reacted.
- (4) When the cBN content is 63 wt%, the relative density, flexural strength and microhardness of the composite are 99%, 820.8 MPa and 3362 Hv, respectively.

## Acknowledgements

This research was financially supported by Key R & D project of Guangxi Province, China (AB20159010).



## References

- [1] Mo PC, Chen JR, Zhang Z, Chen C, Pan XY, Xiao LY (2021) The effect of cBN volume fraction on the performance of PCBN composite. *Int J Refract Met Hard Mater* 100:105643. <https://doi.org/10.1016/j.ijrmhm.2021.105643>
- [2] Li QL, Zhao YB, Sun K, Ji HJ, Feng DD, Li ZH (2018) Composition, microstructure and mechanical properties of cBN-based composites sintered with AlN-Al-Ni binder. *Ceram Int* 44(14):16915–16922. <https://doi.org/10.1016/j.ceramint.2018.06.130>
- [3] Mo PC, Chen C, Jia G, Chen JR, Xie DL, Xiao LY, Pan XY, Lin F (2019) Effect of tungsten content on microstructure and mechanical properties of PCBN synthesized in cBN-Ti-Al-W system. *Int J Refract Met Hard Mater* 87(14):105138. <https://doi.org/10.1016/j.ijrmhm.2019.105138>
- [4] Fiorini P, Byrne G (2016) The influence of built-up layer formation on cutting performance of GG25 grey cast iron. *CIRP Ann* 65(1):93–96. <https://doi.org/10.1016/j.cirp.2016.04.045>
- [5] Gutnichenko O, Bushlya V, Zhou J, Jan-Eric S (2017) Tool wear and machining dynamics when turning high chromium white cast iron with PCBN tools. *Wear* 390:253–269. <https://doi.org/10.1016/j.wear.2017.08.005>
- [6] Ren Z, Qu S, Zhang Y, Sun FJ, Li XQ, Yang C (2019) Machining performance of PCD and PCBN tools in dry turning titanium alloy Ti-6Al-06Cr-04Fe-0.4Si-0.01B. *Int J Adv Manuf Tech* 102(5):2649–2661. <https://doi.org/10.1007/s00170-018-3074-7>
- [7] Diaz J, Criado V, Migulez H, José LC (2018) PCBN performance in high speed finishing turning of inconel 718. *Metals* 8(8):582. <https://doi.org/10.3390/met8080582>
- [8] Chen Z, Lin PR, Zhou J, David G, Johan M (2019) Effect of machining parameters on cutting force and surface integrity when high-speed turning AD 730<sup>TM</sup> with PCBN tools. *Int J Adv Manuf Tech* 100(9):2601–2615. <https://doi.org/10.1007/s00170-018-2792-1>
- [9] Mettaya K, Akihiko I, Zhang JF (2014) Densification and mechanical properties of cBN-TiN-TiB<sub>2</sub> composites prepared by spark plasma sintering of SiO<sub>2</sub>-coated cBN powder. *J Eur Ceram Soc* 34:3619–3626. <https://doi.org/10.1016/j.jeurceramsoc.2014.05.018>
- [10] Liu Y, He D, Wang P et al (2016) Microstructural and mechanical properties of cBN-Si composites prepared from the high pressure infiltration method. *Int J Refract Met Hard Mater* 61:1–5. <https://doi.org/10.1016/j.ijrmhm.2016.07.020>
- [11] Zhang L, Kou ZL, Xu C, Wang KX, Liu CL, Hui B, He DW (2012) Sintering behaviors of fine-grained cBN-10wt.% Al<sub>3,21</sub>Si<sub>0,47</sub> system under high pressure. *Diam Relat Mater* 29:84–88. <https://doi.org/10.1016/j.diamond.2012.08.001>
- [12] Yu WL, Wang JL, Wu Y, Zou ZG, Yu QF, Mo PC (2017) In situ synthesis of polycrystalline cubic boron nitride with high mechanical properties using rod-shaped TiB<sub>2</sub> crystals as the binder. *Adv Appl Ceram* 116(10):1–9. <https://doi.org/10.1080/17436753.2017.1343781>
- [13] Kong F, Yi M, Xiao G et al (2022) Synthesis and characterization of cBN-Al<sub>2</sub>O<sub>3</sub>-Al cutting tool material by dual power spark plasma sintering. *Int J Refract Met Hard Mater* 103:105765. <https://doi.org/10.1016/j.ijrmhm.2021.105765>
- [14] Ji H, Li ZH, Sun K, Zhu YM (2019) Assessment of the performance of TiB<sub>2</sub> nanoparticles doped cBN-TiN-Al-Co composites by high temperature high pressure sintering. *Mater Chem Phys* 233:46–51. <https://doi.org/10.1016/j.materchemphys.2019.05.042>
- [15] Jiang ZL, Jian Q, Han Y, Zhu YM, Li ZH (2020) Performance evaluation of cBN-Ti<sub>3</sub>AlC<sub>2</sub>-Al composites fabricated by HTHP method. *Ceram Int* 46(15):24449–24453. <https://doi.org/10.1016/j.ceramint.2020.06.228>
- [16] Benko E, Klimczyk P, Morgiel J, Włochowicz A, Barrd TL (2003) Electron microscopy investigations of the cBN-Ti compound composites. *Mater Chem Phys* 81(2003):336–340. [https://doi.org/10.1016/S0254-0584\(03\)00016-6](https://doi.org/10.1016/S0254-0584(03)00016-6)
- [17] Zou WJ, Hao DH, Peng J, Dong QM, Li BY, Zhu JF (2011) Performance of PCBN with Si<sub>3</sub>N<sub>4</sub>-Ni binder and application of the PCBN turning tool. *Diam Abra Eng* 41(03):19–22. <https://doi.org/10.1016/10.13394/j.cnki.jgszz.2021.3.0003>
- [18] Yu L, Zi LK, Wang HK, Wang KX et al (2012) High pressure sintering behavior and mechanical properties of cBN-Ti<sub>3</sub>Al and cBN-Ti<sub>3</sub>Al-Al composite materials. *High Press Res* 32(4):524–531. <https://doi.org/10.1080/08957959.2012.736507>
- [19] Mckie A, Winzer J, Sigalas I, Mathias H, Ludwig W, Jürgen R, Nedret C (2011) Mechanical properties of cBN-Al composite materials. *Ceram Int* 37(1):1–8. <https://doi.org/10.1016/j.ceramint.2010.07.034>
- [20] Zhang LL, Lv Z, Lin F et al (2015) cBN-Al-HfC composites: Sintering behaviors and mechanical properties under high pressure. *Int J Refract Met Hard Mater* 50:221–226. <https://doi.org/10.1016/j.ijrmhm.2015.01.015>
- [21] Li ML, Liang LX, Wang HL, Zhao PB, Zhao XT, Shao G, Zhang R (2020) Processing and properties of PcBN composites fabricated by HPHT using PSN and Al as sintering additive. *Rare Met* 39(05):570–576. <https://doi.org/10.1007/s12598-020-01371-y>
- [22] Mo PC, Wu Y, Yu WL, Wang JL, Zou ZG, Zhong SL, Wang P (2018) In situ synthesis of PcBN composites by cBN/Ti/Al/Si and the mechanical property of research. *Mater Rev* 32(14):30–34. <https://doi.org/10.11896/j.issn.1005-023X.2018.14.006>

- [23] Yuan Y, Cheng X, Chang R et al (2016) Reactive sintering cBN-Ti-Al composites by spark plasma sintering. *Diam Relat Mater* 69:138–143. <https://doi.org/10.1016/j.diamond.2016.08.009>
- [24] Wang B, Qin Y, Jin F, Yang JF, Kozo I (2014) Pulse electric current sintering of cubic boron nitride/tungsten carbide-cobalt (cBN/WC–Co) composites: effect of cBN particle size and volume fraction on their microstructure and properties. *Mater Sci Eng A* 607:490–497. <https://doi.org/10.1016/j.msea.2014.04.029>
- [25] Zhang CP, Gao XW, Ru HQ, Sun WK, Zhu JH, Zong H (2017) Effect of forming pressure on microstructure and mechanical properties of SiC/TiB<sub>2</sub> composites. *J Inorg Mater* 32(05):502–508. <https://doi.org/10.15541/jim20160429>
- [26] Hu HL, Yao DX, Xia YF, Zou KH, Zeng YP (2014) Mechanical properties of reaction-bonded Si<sub>3</sub>N<sub>4</sub>/SiC composite ceramics. *J Inorg Mater* 29(06):594–598. <https://doi.org/10.3724/SP.J.1077.2014.13469>
- [27] Xiao SQ, Liu J, Xiao BJ, Deng X, Wu SH (2018) Towards high strength and high toughness Ti(CN)-based cermets: a technological review. *Mater Rev* 32(07):1129–1138. <https://doi.org/10.11896/j.issn.1005-023X.2018.07.013>

**Publisher's Note** Springer Nature remains neutral with regard to jurisdictional claims in published maps and institutional affiliations.

Springer Nature or its licensor holds exclusive rights to this article under a publishing agreement with the author(s) or other rightsholder(s); author self-archiving of the accepted manuscript version of this article is solely governed by the terms of such publishing agreement and applicable law.